Supplementary Information
Designing two-photon molecular emitters in nanoparticle-on-mirror cavities

S. Smeets,[1] B. Maes,[1] G. Rosolen,[1] and C. Van Dyck[2]

[1] *Micro- and Nanophotonic Materials Group, Research Institute for Materials Science and Engineering, University of Mons, 20 Place du Parc, Mons B-7000, Belgium*

[2] *Theoretical Chemical Physics Group, Research Institute for Materials Science and Engineering, University of Mons, 20 Place du Parc, Mons B-7000, Belgium*

(Dated: August 27, 2025)

I. COMPARISON BETWEEN TD-DFT AND PPP RESULTS

In Table I are provided the results obtained via TD-DFT (QRDR formalism) and via PPP model. The conclusions are discussed in the main text.

Method	Molecule	ΔE_{10} [eV]	ΔE_{21} [eV]	$\mathcal{D}^{eg}(0.5)$ [a.u.]	$\phi_0^{(2)}(0.5)$ $[\mathrm{s}^{-1}]$	$\Gamma_0^{(2)}$ $[\mathrm{s}^{-1}]$
DFT	DPB	3.43	0.17	10.3	9.30×10^{-2}	2.82×10^{-2}
	DPH	2.55	0.40	49.8	4.96×10^{-1}	1.34×10^{-1}
	NO_2-OPPV	2.92	0.10	83.8	2.76	8.54×10^{-1}
PPP	DPB	2.44	0.17	99.8	1.59	4.48×10^{-1}
	DPH	2.37	0.40	104	1.50	4.10×10^{-1}
	NO_2-OPPV	2.47	0.10	218	8.17	2.64

TABLE I. **TD-DFT and PPP results**. For TD-DFT, the energy gap ΔE_{21} is calculated using the PPP model and used to correct the energy of the $2A_g$ state (first excited state). ΔE_{10} and ΔE_{21} are, respectively, the energy gaps between the first excited state ($2A_g$) and the ground state ($1A_g$), between the second excited state ($1B_u$) and the first excited state ($2A_g$). $\mathcal{D}^{eg}(0.5)$ is the norm of the second-order transition moment for $\nu = 0.5$ and a TPSE transition from first excited state ($2A_g$) to the ground state ($1A_g$). $\phi_0^{(2)}$ and $\Gamma_0^{(2)}$ are, respectively, the vacuum spectral TPSE rate at $\nu = 0.5$ and the integrated vacuum TPSE rate.

II. COMPARISON BETWEEN DIFFERENT TD-DFT THEORY LEVELS

In Table II are provided the results obtained via different TD-DFT theory levels. The conclusions are discussed in the main text.

III. SIMULATION PARAMETERS

We use the COMSOL Multiphysics® software [1] based on the finite element method to compute the Purcell factors over a range of frequencies [2]. The simulation domain is a sphere with a radius equal to twice the studied wavelength λ, and perfectly matched layers (PMLs) are defined as an outer layer with a thickness of $\lambda/2$. Moreover, the tip of the gold nanocone has rounded edges with a diameter equal to 30% of $D_2 = 6$ nm and the gold optical response is given by a Lorentz-Drude model [3]. The classical emitter is positioned in the middle of the gap and is modelled by an electric point dipole oscillating along the cone axis. The Purcell factors are determined through the integration of emitted power on the inner surface of the PMLs for the radiative part and on the surface of a fictional sphere with a 1 nm radius centred on the emitter for the total part (sum of radiative and non-radiative parts). The entire domain is meshed with unstructured tetrahedra, except in the spacer, where 6 layers with a triangular prism mesh are

Molecule	TD-DFT theory levels	ΔE_{10} [eV]	ΔE_{21} [eV]	$\mathcal{D}^{eg}(0.5)$ [a.u.]	$\phi_0^{(2)}(0.5)$ $[s^{-1}]$	$\Gamma_0^{(2)}$ $[s^{-1}]$
DPB	B3LYP/6-31G*	3.27	0.17	17.2	2.06×10^{-1}	6.42×10^{-2}
	CAM-B3LYP/6-31G*	3.53	0.17	9.03	8.26×10^{-2}	2.22×10^{-2}
	CAM-B3LYP/6-31+G*	3.43	0.17	10.3	9.30×10^{-2}	2.82×10^{-2}
DPH	B3LYP/6-31G*	2.44	0.40	35.5	2.03×10^{-1}	5.44×10^{-2}
	CAM-B3LYP/6-31G*	2.63	0.40	53.5	6.60×10^{-1}	1.78×10^{-1}
	CAM-B3LYP/6-31+G*	2.55	0.40	49.8	4.96×10^{-1}	1.34×10^{-1}
NO_2-OPPV	B3LYP/6-31G*	2.55	0.10	122	3.00	9.51×10^{-1}
	CAM-B3LYP/6-31G*	3.03	0.10	77.2	2.82	8.77×10^{-1}
	CAM-B3LYP/6-31+G*	2.92	0.10	83.8	2.76	8.54×10^{-1}

TABLE II. **TD-DFT results for three theory levels.** The geometry is optimized using CAM-B3LYP/6-31G* for all TD-DFT theory levels. The energy gap ΔE_{21} is calculated using the PPP model and used to correct the energy of the $2A_g$ state (first excited state). ΔE_{10} and ΔE_{21} are, respectively, the energy gaps between the first excited state ($2A_g$) and the ground state ($1A_g$), between the second excited state ($1B_u$) and the first excited state ($2A_g$). $\mathcal{D}^{eg}(0.5)$ is the norm of the second-order transition moment for $\nu = 0.5$ and a TPSE transition from first excited state ($2A_g$) to the ground state ($1A_g$). $\phi_0^{(2)}$ and $\Gamma_0^{(2)}$ are, respectively, the vacuum spectral TPSE rate at $\nu = 0.5$ and the integrated vacuum TPSE rate.

employed. The smallest element has a characteristic size of 0.08 nm on the structure and on the sphere around the emitter. Calculating the Purcell factor P_x over 95 frequencies for the system optimised for the NO_2-OPPV molecule requires 100 GB of RAM and 24 hours using 12 cores of an AMD Ryzen Threadripper PRO 5995WX CPU.

IV. COMPARISON OF NANOPARTICULE GEOMETRIES

We compare various nanoparticle geometries [Fig.1] to enhance the emission from the NO2-OPPV molecule, which has a transition energy of $\hbar\omega_{eg} = 2.92$ eV. The particle dimensions are optimised to maximize emission at half the transition frequency. For conical particles, we additionally investigate the influence of tip size and the absence of the mirror [4]. The corresponding results are presented in Table III and Figure 2, with detailed conclusions discussed in the main text.

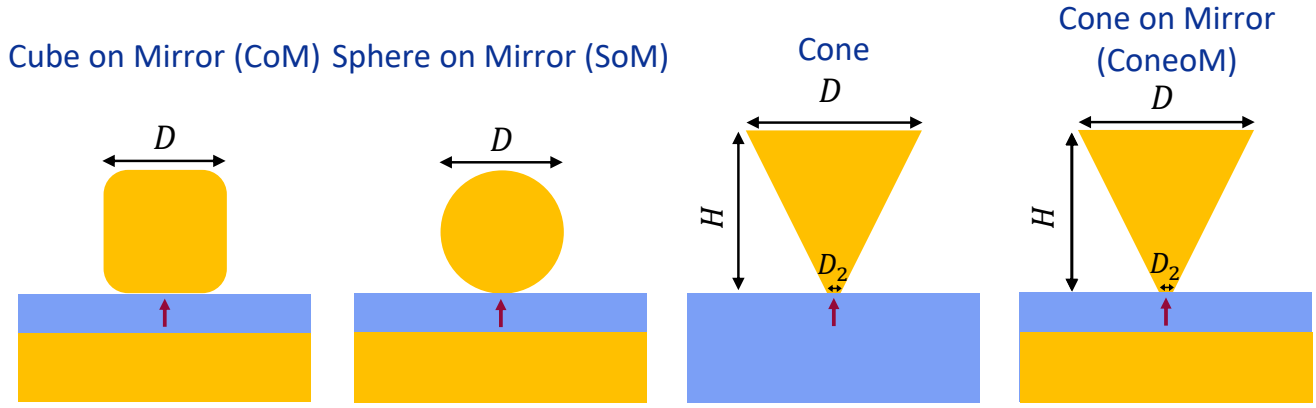

FIG. 1. **Schematic representation of the four studied nanocavities.** Blue regions indicate the spacer material ($n = 1.4$), while yellow regions represent gold.

[1] COMSOL Multiphysics® v. 6.3., www.comsol.com. COMSOL AB, Stockholm, Sweden.
[2] S. Smeets, *Analytical and numerical investigation of the two-photon spontaneous emission process near plasmonic nanostructures*, Ph.D. thesis, University of Mons, Belgium (2024).

Structure	D [nm]	H [nm]	D_2 [nm]	$\phi^{(2)}_{\text{ph-ph}}(0.5)/\phi^{(2)}_0(0.5)$	$\phi^{(2)}_{\text{ph-ph}}(0.5)$ [s^{-1}]	$\Gamma^{(2)}_{\text{ph-ph}}$ [s^{-1}]	$\eta^{(2)}$	ξ
CoM	132			9.85×10^7	2.72×10^8	7.51×10^6	3.80%	2.84×10^{-1}
SoM	142			6.79×10^7	1.87×10^8	1.63×10^7	11.7%	6.14×10^{-1}
Cone	120	265	6.0	6.26×10^8	1.72×10^9	5.21×10^7	38.0%	1.97
Cone	120	265	4.0	2.43×10^9	6.70×10^9	2.00×10^8	36.5%	7.56
ConeoM	95	130	6.0	1.69×10^{10}	4.67×10^{10}	1.41×10^9	40.5%	55.3
ConeoM	95	130	4.0	2.72×10^{10}	7.50×10^{10}	2.19×10^9	35.9%	82.8

TABLE III. **Results of the two-photon enhancement with different particle geometries for the NO_2-OPPV molecule.** The gap size is fixed at 3 nm for all systems. The quantity $\phi^{(2)}_{\text{ph-ph}}(0.5)/\phi^{(2)}_0(0.5)$ denotes the enhancement of the two-photon emission rate into the far field compared to vacuum, evaluated at $\nu = 0.5$. $\Gamma^{(2)}_{\text{ph-ph}}$ corresponds to the integrated two-photon emission rate. $\eta^{(2)}$ is quantum efficiency, defined as the probability of emitting a photon pair into the far-field. $\xi := \Gamma^{(2)}_{\text{ph-ph}}/\Gamma^{(1)}_0$, with $\Gamma^{(1)}_0 = \omega^3_{eg} \|\mathbf{d}^{eg}\|^2 / 3\pi\varepsilon_0\hbar c^3$ [5], quantifies the enhancement of the two-photon emission rate with respect to the vacuum one-photon emission rate of an emitter with a transition dipole moment $\mathbf{d}^{eg}$ of one atomic unit.

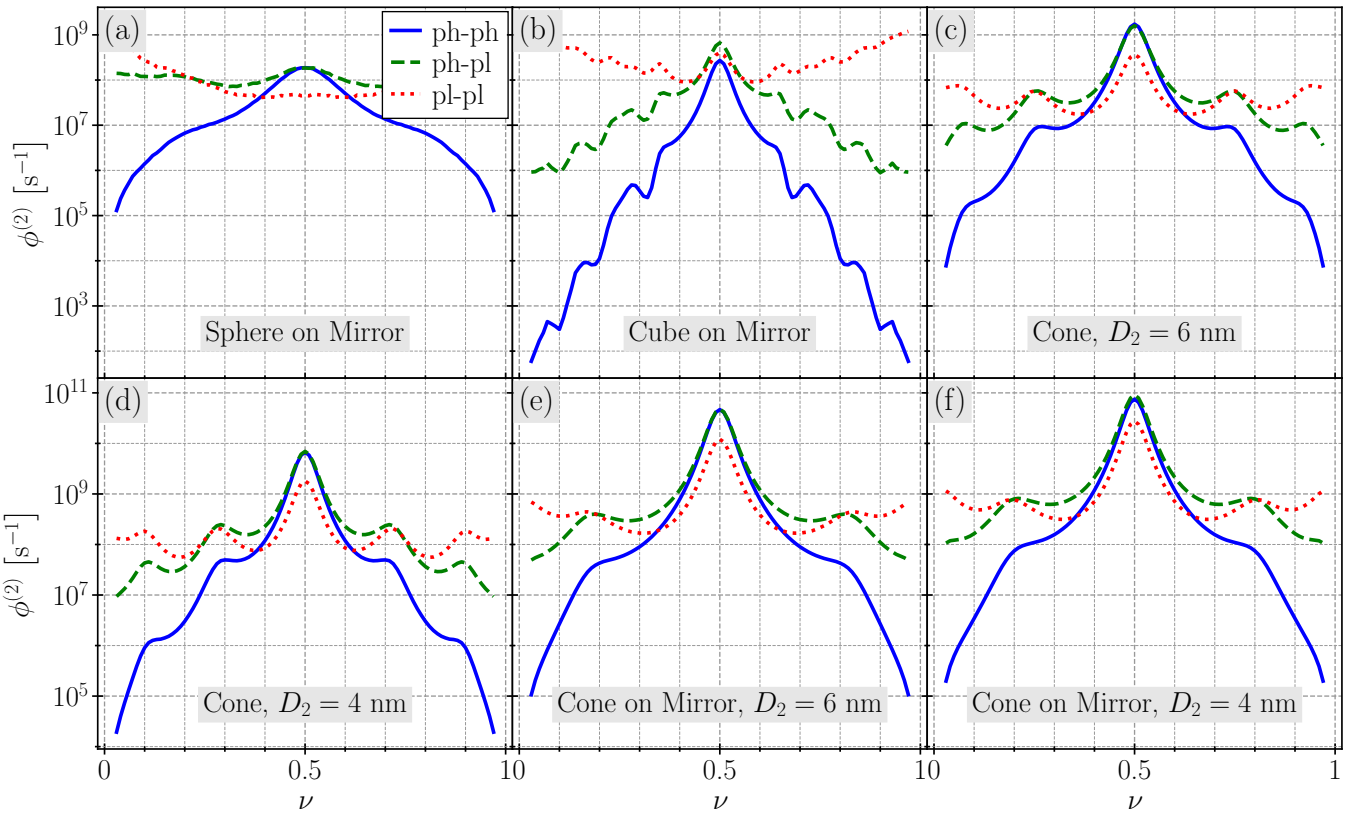

FIG. 2. Photon-photon, photon-plasmon, and plasmon-plasmon emission channels of the spectral two-photon spontaneous emission rate of the NO_2-OPPV molecule placed in six different nanocavities. The spectrum for the TSoM cavity is similar to that of the SoM cavity.

[3] A. D. Rakić, A. B. Djurišić, J. M. Elazar, and M. L. Majewski, Optical properties of metallic films for vertical-cavity optoelectronic devices, Applied Optics **37**, 5271 (1998).

[4] X.-W. Chen, M. Agio, and V. Sandoghdar, Metallodielectric hybrid antennas for ultrastrong enhancement of spontaneous emission, Physical Review Letters **108**, 233001 (2012).

[5] D. P. Craig and T. Thirunamachandran, *Molecular quantum electrodynamics: an introduction to radiation-molecule interactions* (Academic Press, London ; Orlando, 1984).